

## Supporting Information

### **Additive-Free Shape-Invariant Nano-to-Micron Size-Tuning of Cu<sub>2</sub>O Cubic Crystals by Square-Wave Voltammetry**

*Xuyun Guo,<sup>1</sup> Weiqiang Lv,<sup>1</sup> and Xiao-Yuan Li<sup>1,2,3\*</sup>*

<sup>1</sup>Department of Chemistry, <sup>2</sup>William Mong Institute of Nano Science and Technology,  
<sup>3</sup>Energy Institute,

The Hong Kong University of Science and Technology,

Clear Water Bay, Kowloon, Hong Kong SAR, People's Republic of China

\* To whom correspondence should be addressed at (852)-2358-7356, Email: chxyli@ust.hk

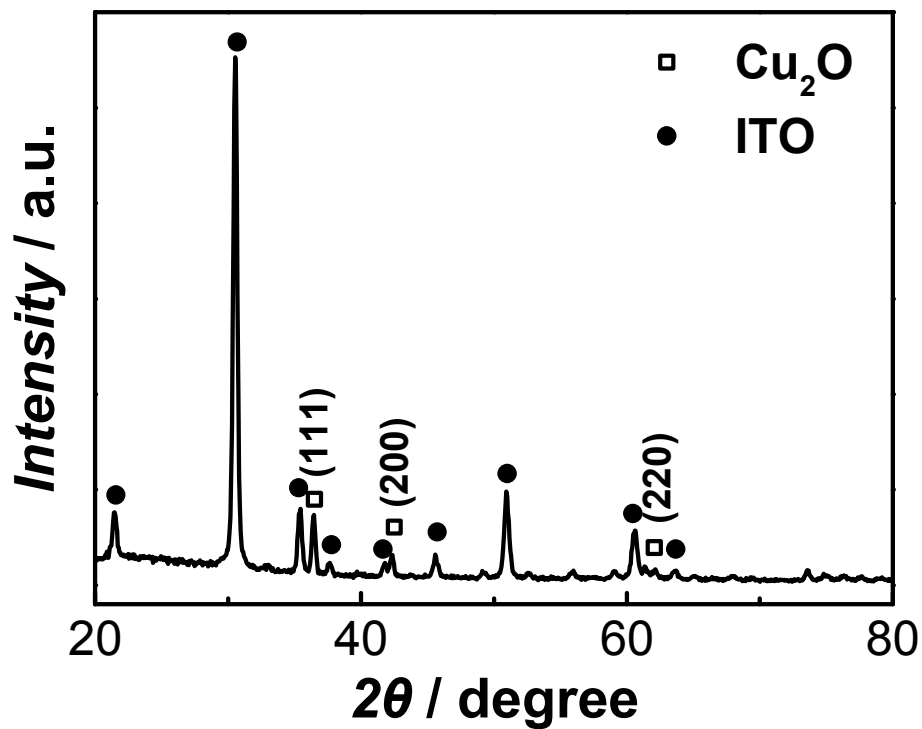


**Figure S1.** A typical XRD pattern of the as-fabricated  $\text{Cu}_2\text{O}$  crystalline nanocubes electrodeposited on an ITO substrate by SWV. The SWV parameters used are  $t_0 = 2$  s,  $f = 6$  Hz,  $E_0 = -0.08$  V,  $E_i = -0.08$  V,  $E_f = -0.20$  V,  $\Delta E_{\text{step}} = -0.333$  mV,  $E_{\text{sw}} = 80$  mV,  $N = 20$ . All peaks are attributable to either  $\text{Cu}_2\text{O}$  crystalline particles or the ITO substrate.

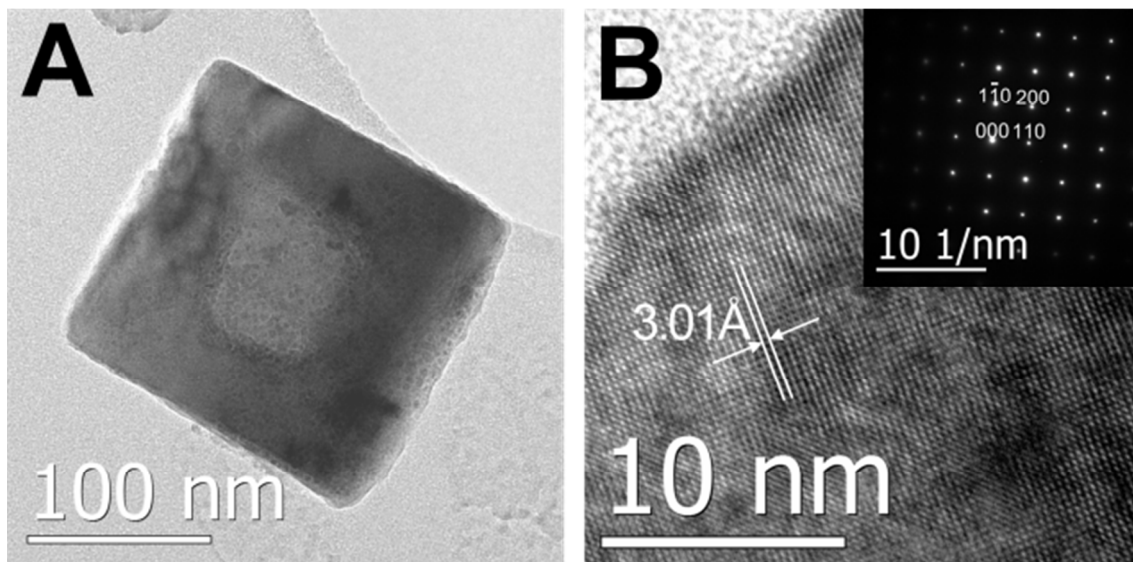


**Figure S2.** ( A ) TEM image of a typical crystalline  $\text{Cu}_2\text{O}$  nanocube from the  $\text{Cu}_2\text{O}$  sample electrodeposited on an ITO substrate by SWV. The SWV parameters used are  $t_0 = 2$  s,  $f = 6$  Hz,  $E_0 = -0.08$  V,  $E_i = -0.08$  V,  $E_f = -0.20$  V,  $\Delta E_{\text{step}} = -0.333$  mV,  $E_{\text{sw}} = 80$  mV,  $N = 5$ . ( B ) HRTEM lattice image near the edge of the  $\text{Cu}_2\text{O}$  nanocube shown in Graph A. The inset in ( B ) shows the SAED pattern in the same region.

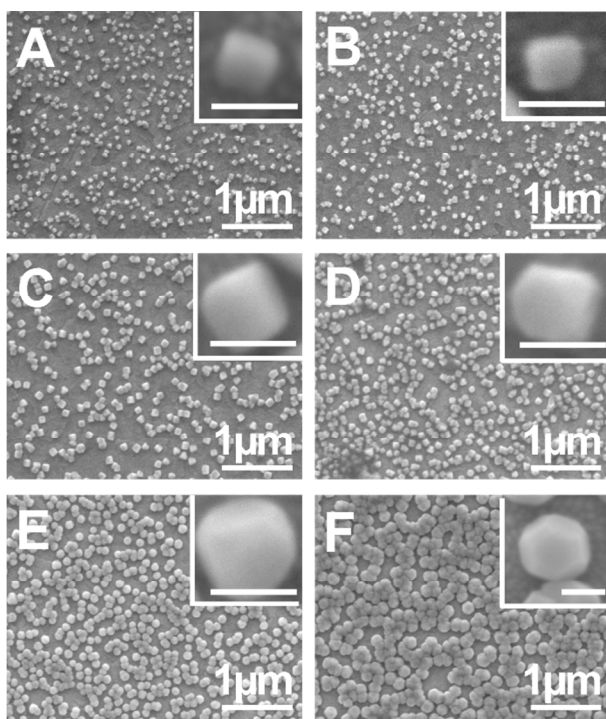


**Figure S3.** SEM images showing the effect of the deposition time (  $t$  ) to the shape and size of the electrodeposited  $\text{Cu}_2\text{O}$  nanocrystals and their coalescence into a film by chronoamperometry ( CA or simple  $i \sim t$  ) method. The CA parameters used are  $t_0 = 2$  s,  $E_0 = -0.2$  V,  $E_i = -0.2$  V.  $t = 1$  ( A ), 3 ( B ), 5 ( C ), 10 ( D ), 20 ( E ), and 40 min ( F ), respectively. The scale bars in the insets represent 100 nm.

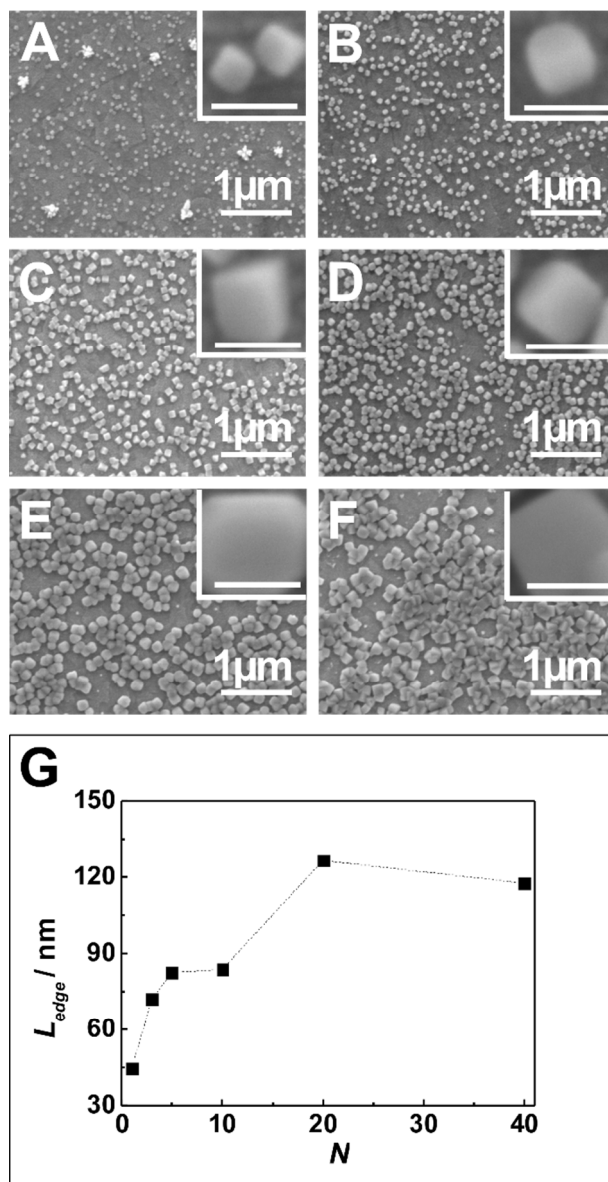


**Figure S4.** SEM images showing the effect of reversing the scan direction in SWV to the nucleation and the size of the electrodeposited  $\text{Cu}_2\text{O}$  nanocubes under the condition of  $|\Delta E_{\text{step}}| \ll E_{\text{sw}}$  and  $|\Delta E_{\text{step}}| \ll |E_f - E_i|$ . The SWV parameters used are same as that of Figure-9, except that  $E_0 = E_i = -0.20$  V and  $E_f = -0.08$  V.  $N = 1$  (A), 3 (B), 5 (C), 10 (D), 20 (E), and 40 (F), respectively. Graph-G shows the size variation of  $\text{Cu}_2\text{O}$  nanocubes when  $N$  was changed from 1 to 40. The scale bars in the insets represent 100 nm.

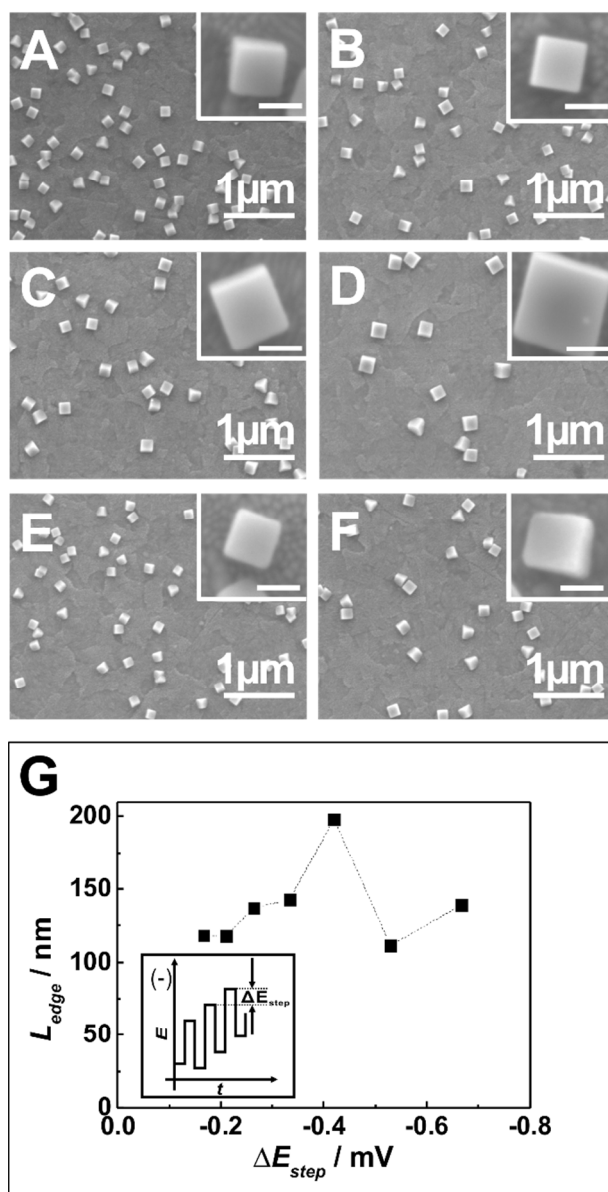


**Figure S5.** SEM images showing the effect of the step potential ( $\Delta E_{\text{step}}$ ) in SWV to the nucleation and the size of the electrodeposited Cu<sub>2</sub>O nanocubes under the condition of  $|\Delta E_{\text{step}}| \ll E_{\text{sw}}$  and  $|\Delta E_{\text{step}}| \ll |E_{\text{f}} - E_{\text{i}}|$ .  $\Delta E_{\text{step}} = -0.167$  (A),  $-0.210$  (B),  $-0.264$  (C),  $-0.420$  (D),  $-0.529$  (E), and  $-0.667$  mV (F), respectively. Graph-G shows the size variation of Cu<sub>2</sub>O nanocubes when  $\Delta E_{\text{step}}$  was changed from  $-0.167$  to  $-0.667$  mV, corresponding to the change of the scan rate from 1 to 4 mV/s. Other SWV parameters are  $t_0 = 2$  s,  $f = 6$  Hz,  $E_0 = -0.08$  V,  $E_{\text{i}} = -0.08$  V,  $E_{\text{f}} = -0.20$  V,  $E_{\text{sw}} = 80$  mV,  $N = 1$ . The scale bars in the insets represent 100 nm.

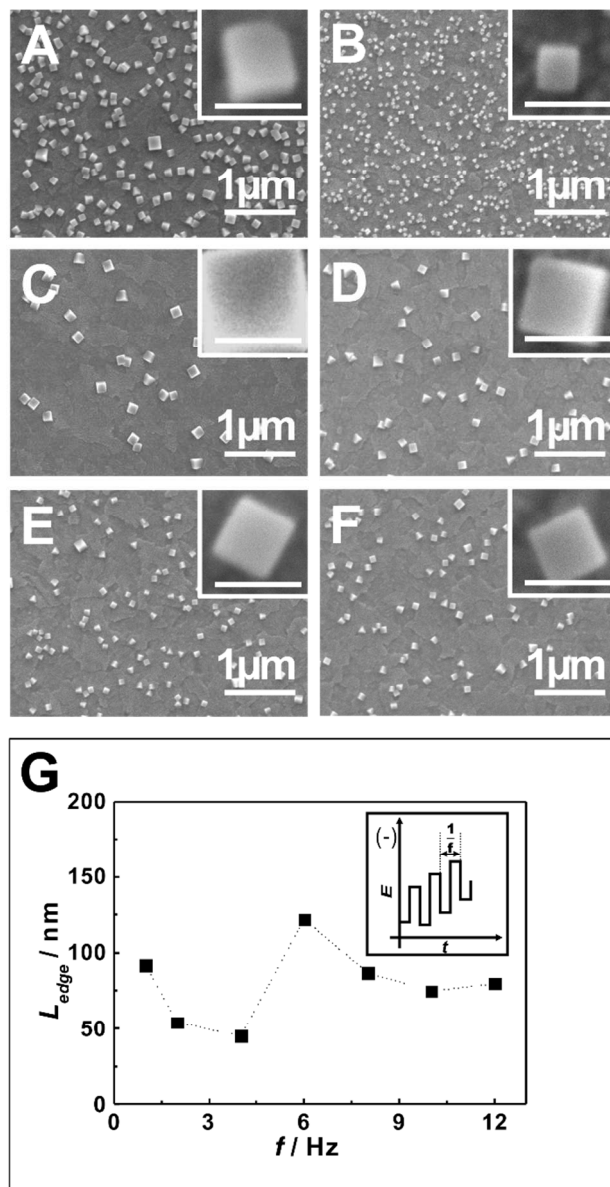


**Figure S6.** SEM images showing the effect of the frequency ( $f$ ) in SWV to the size of the electrodeposited Cu<sub>2</sub>O nanocubes under the condition of  $|\Delta E_{\text{step}}| \ll E_{\text{sw}}$  and  $|\Delta E_{\text{step}}| \ll |E_f - E_i|$ .  $f = 1$  (A), 4 (B), 6 (C), 8 (D), 10 (E) and 12 Hz (F), respectively. Graph-G shows the size variation of the deposited Cu<sub>2</sub>O nanocubes when  $f$  is changed from 1 to 12 Hz. Other SWV parameters are  $t_0 = 2$  s,  $E_0 = -0.08$  V,  $E_i = -0.08$  V,  $E_f = -0.20$  V,  $\Delta E_{\text{step}} = -0.333$  mV,  $E_{\text{sw}} = 80$  mV,  $N = 1$ . The scale bars in the insets represent 100 nm.

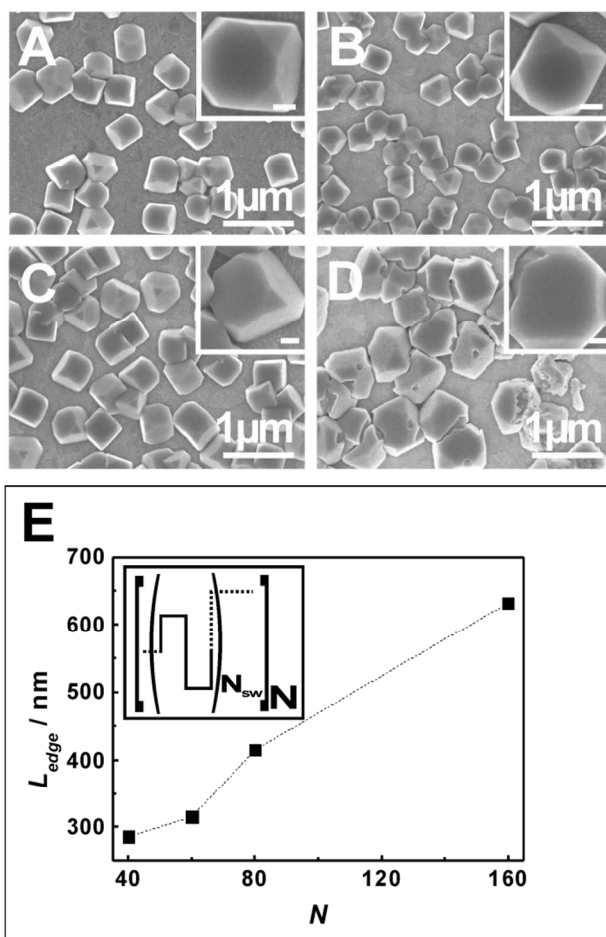


**Figure S7.** Same as Figure 9 except  $N = 40$  (A), 60 (B), 80 (C), and 160 (D), respectively. Graph-E shows the size variation of the deposited Cu<sub>2</sub>O nanocubes when  $N$  is changed from 40 to 160. With the increase of  $N$ , the shape of the electro-deposited Cu<sub>2</sub>O particles deviates considerably from that of cube. The deposited Cu<sub>2</sub>O particles eventually coalesce into a film with the cracks formed from the inter-particle boundaries. The scale bars in the insets represent 100 nm.

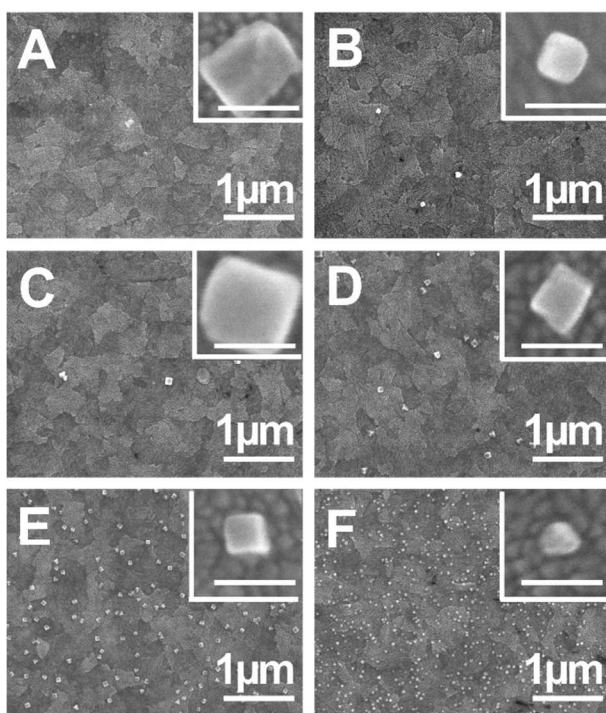


**Figure S8.** SEM images showing the effect of the set potential (  $E_0$  ) to the seeding of  $\text{Cu}_2\text{O}$  before any SWV pulses were applied.  $E_0$  ( *vs.* SCE ) = 0.04 ( A ), -0.02 ( B ), -0.06 ( C ), -0.10 ( D ), -0.14 ( E ), and -0.20 V ( F ), respectively.  $t_0 = 2$  s. The scale bars in the insets represent 100 nm.

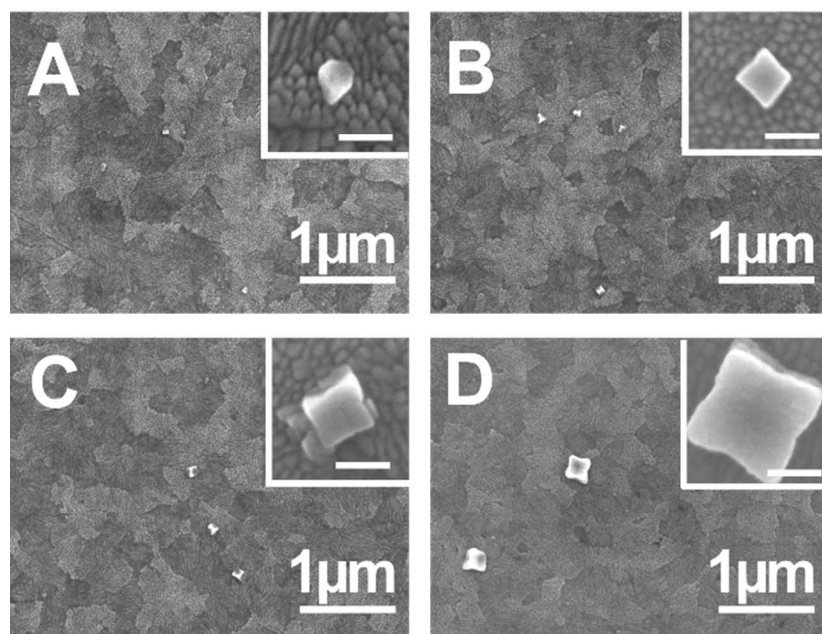


**Figure S9.** SEM images showing the effect of the waiting time ( $t_0$ ) at  $E_0$  to the seeding of  $\text{Cu}_2\text{O}$  before any SWV pulses were applied.  $t_0 = 1$  ( A ), 2 ( B ), 3 ( C ), 5 s ( D ), respectively.  $E_0 = -0.08$  V. The scale bars in the insets represent 100 nm.

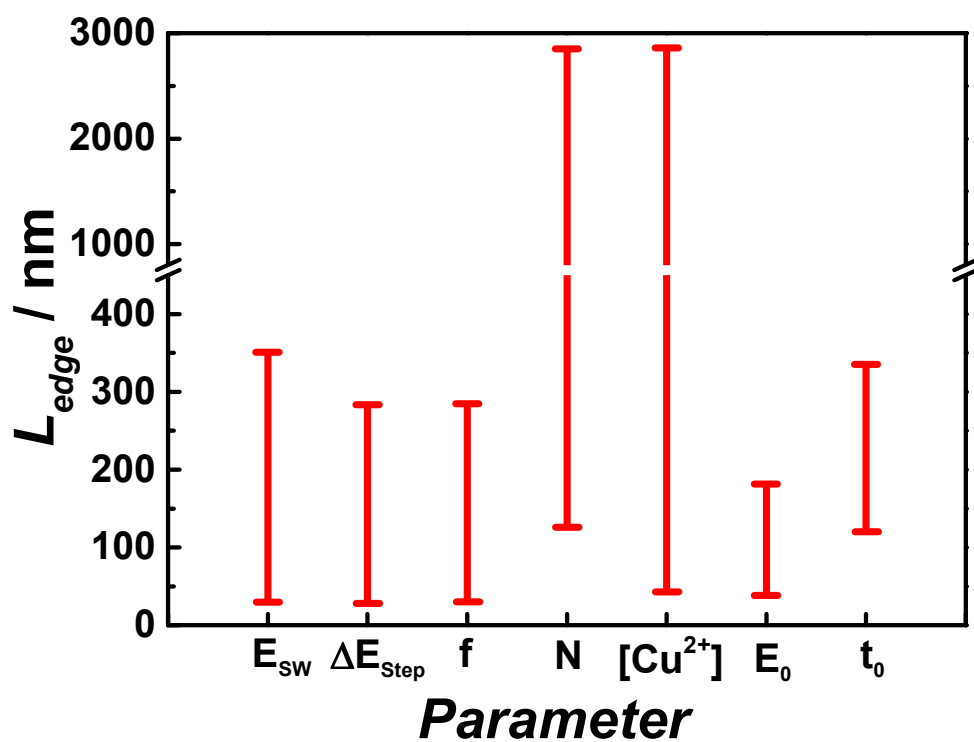


**Figure S10.** Graph illustrating the shape-invariant size-tunable ranges of the electrodeposited  $Cu_2O$  nanocubes by adjusting individual parameters in SWV examined in this study. The data were from Figure-5 for  $E_{sw}$ , Figure 11-A for  $\Delta E_{step}$ , Figure 11-B for  $f$ , Figure 11-D for  $N$ , Figures 10 and 11-D for  $[Cu^{2+}]$ , Figure 14 for  $E_0$ , and Figure 15 for  $t_0$ , respectively.

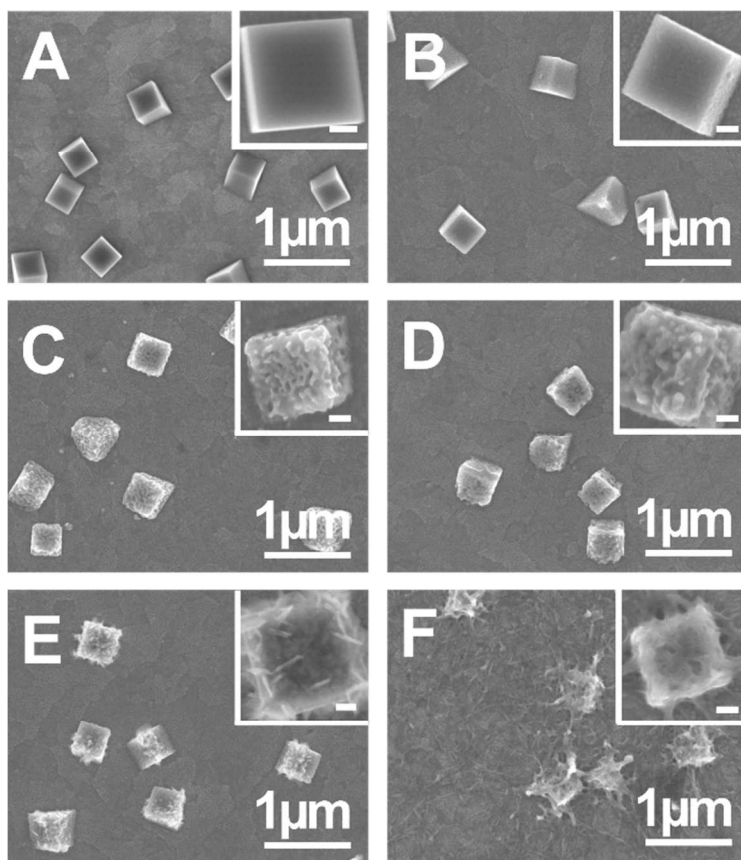


**Figure S11.** SEM images showing the effect of the time used in the galvanic displacement reaction to the structure of the fabricated  $\text{Cu}_2\text{O}@\text{Ag}$  composites. The reaction time is 0 ( A ), 0.5 ( B ), 1 ( C ), 2 ( D ), 3 ( E ) and 4 hours ( F ), respectively, in 1 mM  $\text{AgNO}_3$  aqueous solution at ambient condition in the dark without any supporting electrolyte. The cubic  $\text{Cu}_2\text{O}$  templates were fabricated by SWV using the same parameters as that of Graph-E in Figure-10. The scale bars in the insets represent 100 nm.

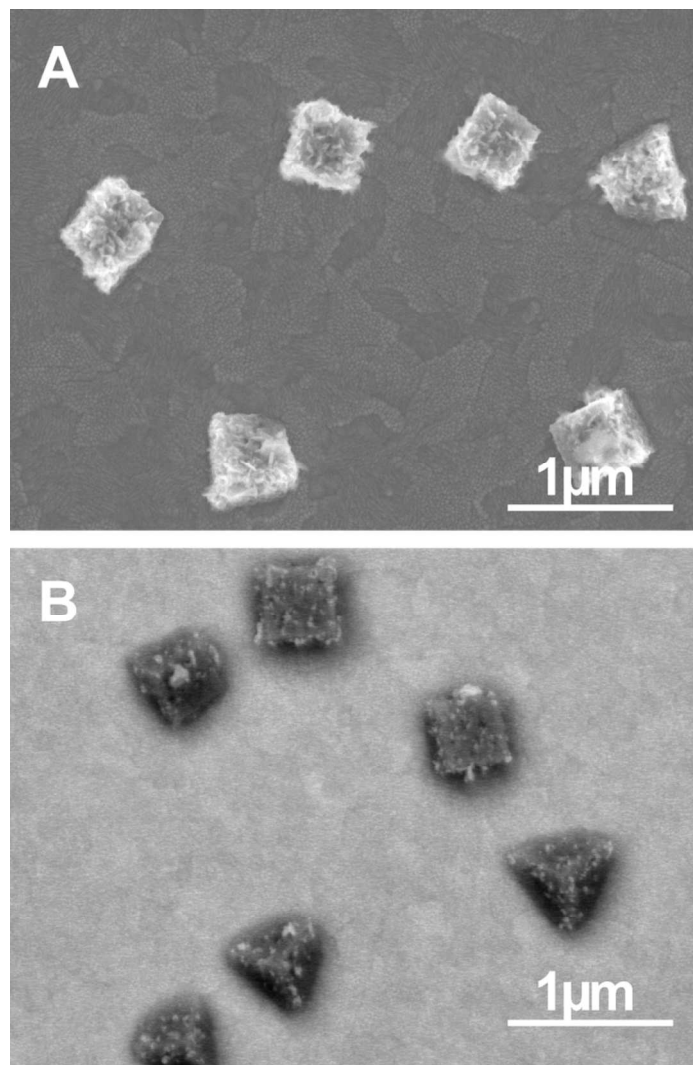


**Figure S12.** SEM images of the  $\text{Cu}_2\text{O}@\text{Ag}$  composites taken by the secondary electron mode ( SEI, **A** ) and the backscattered electron mode ( BEI, **B** ) to examine the morphology and the composition of the as-fabricated  $\text{Cu}_2\text{O}@\text{Ag}$ , respectively. The  $\text{Cu}_2\text{O}@\text{Ag}$  sample was fabricated using the same conditions as that for Graph E, Figure-S11.

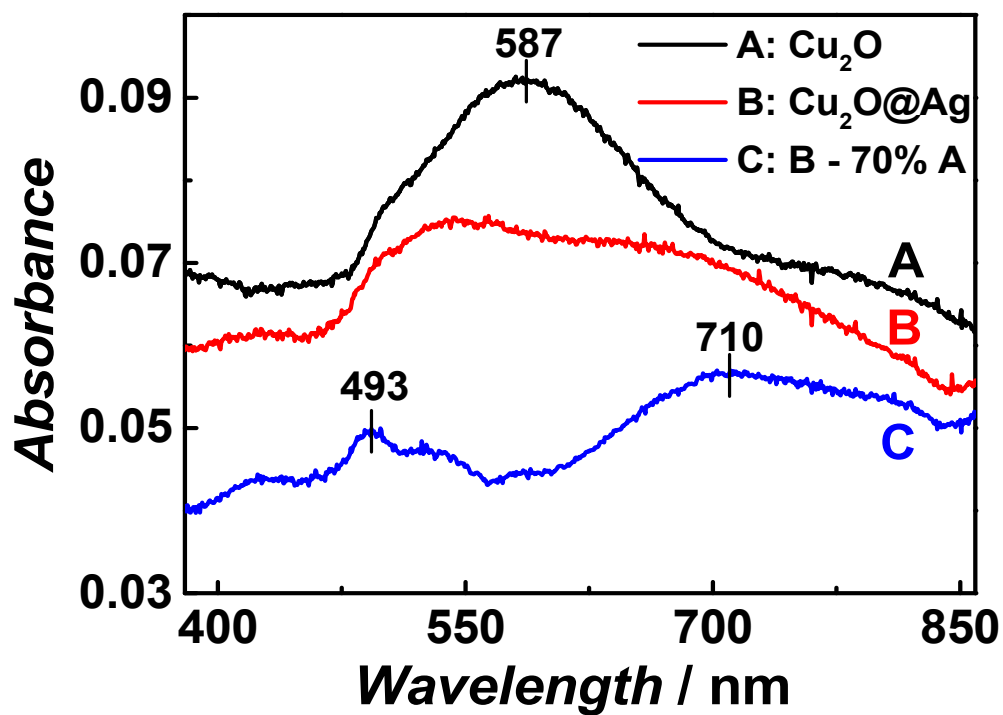


**Figure S13.** UV-Vis-NIR spectra of the Cu<sub>2</sub>O cubic nano-templates ( A ), Cu<sub>2</sub>O@Ag composites ( B ), and the estimated contribution from the Ag shell ( C = B - 70%A ). The Cu<sub>2</sub>O and Cu<sub>2</sub>O@Ag samples were fabricated using the same parameters as that for Graph E, Figure-S11.